

# Growth of uniformly aligned nanorod arrays by oblique angle deposition with two-phase substrate rotation

D-X Ye<sup>1,3</sup>, T Karabacak<sup>1</sup>, B K Lim<sup>2</sup>, G-C Wang<sup>1</sup> and T-M Lu<sup>1</sup>

<sup>1</sup> Department of Physics, Applied Physics, and Astronomy, Rensselaer Polytechnic Institute, Troy, NY 12180-3590, USA

<sup>2</sup> Department of Materials Engineering, Nanyang Technological University, 639798, Singapore

E-mail: yed@rpi.edu

Received 8 March 2004

Published 26 April 2004

Online at [stacks.iop.org/Nano/15/817](http://stacks.iop.org/Nano/15/817)

DOI: 10.1088/0957-4484/15/7/018

## Abstract

Due to the shadowing effect, the oblique angle deposition technique can produce nanorods tilted toward the incident deposition flux. Periodic posts serving as seeds on a substrate allow the fabrication of nanorod arrays with controllable separations. However, in a conventional oblique angle deposition with *no* substrate rotation, nanorods grow faster along their widths in the direction perpendicular to the plane of incident flux. This anisotropic growth can result in ‘fan-out’ shapes of nanorods that touch each other due to the faster growing widths. Asymmetric two-phase substrate rotation was designed to eliminate the side growth in oblique angle deposition. In this method, the growing rods are exposed to the deposition flux from all angles with some portion of a rod surface receiving more flux than the rest. We fabricated well-aligned Si nanorod arrays with uniform sizes from templates arranged in square and triangular lattices using this two-phase substrate rotation method.

## 1. Introduction

Nanorods are believed to be one of the most important building blocks for the assembly of integrated nano-electrical, nano-optical and nano-mechanical systems. They are also of great interest as individual nanodevices including nanoelectronics [1–3], field emitters [4, 5], nano-optics [6], photonic crystals [7] and gas sensors [8]. Therefore fundamental studies of the physical and chemical properties of nanorods were required to understand the benefits and limits of these materials. Despite the achievements obtained recently in studying the mechanical [9, 10], electrical [11] and optical [12, 13] properties of nanorods, a better understanding of many issues related to these properties is limited by the ability of fabricating spatially separated nanorods with controllable sizes and geometries. Tilted nanorods are preferred in these studies due to the anisotropic nature inherent

within the tilted geometry. However, this structure cannot be easily fabricated by lithographic methods or chemical self-assembly processes. In this paper, we propose a new approach to create separated and well-aligned nanorod arrays using the oblique angle deposition technique combined with a two-phase substrate rotation. This new method can produce uniformly aligned slanted nanorods with a controllable tilt angle. The nanostructures obtained by this method are particularly useful in the study of their mechanical bending, the electrical and optical responses to the external excitations from an atomic force microscope (AFM) tip. They can also be used as a backbone for functionalizing the surface in chemical and biological sensing systems.

In a conventional oblique angle deposition technique [14–16], the vapour atoms travel to a fixed substrate at a large oblique angle  $\theta$  ( $70^\circ$ – $90^\circ$ ) relative to the surface normal of the substrate. This technique has been shown to be an efficient approach to fabricate nanorod structures with each rod tilting toward the incident flux [17]. The tilting angle  $\beta$

<sup>3</sup> Author to whom any correspondence should be addressed.

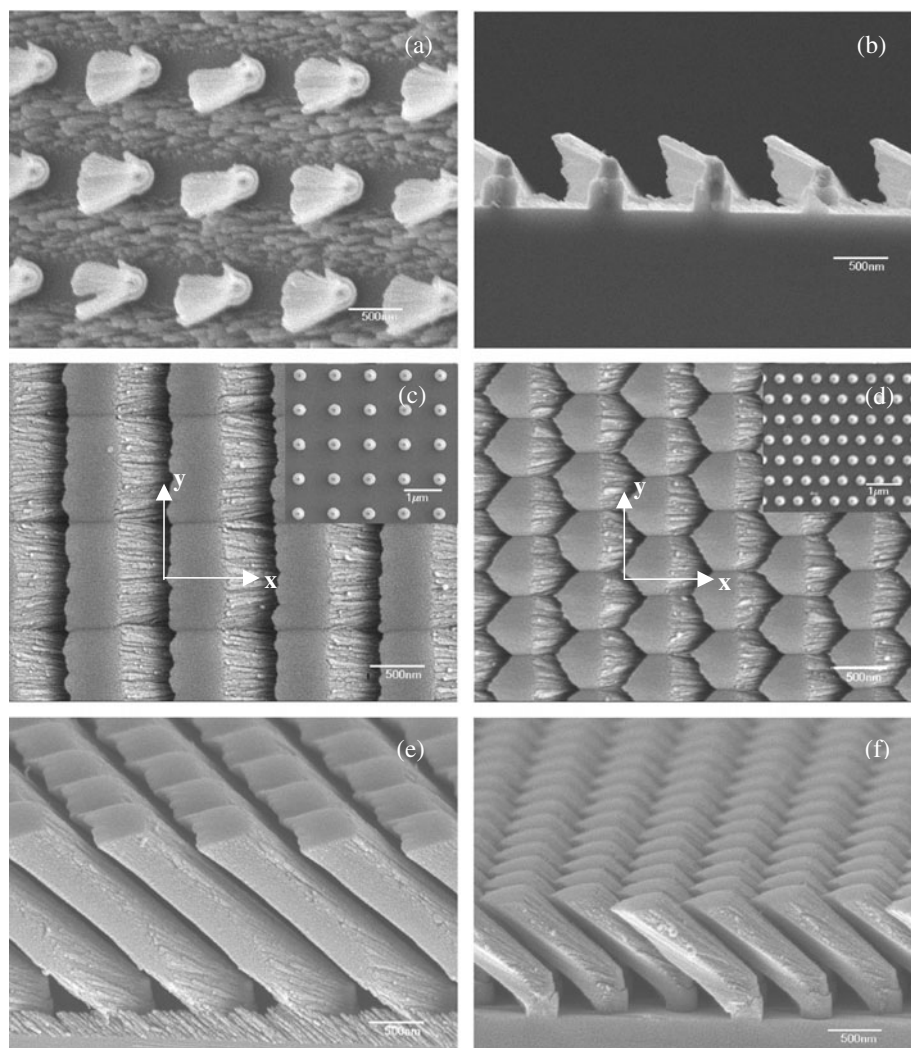


**Figure 1.** SEM images of the nanostructures created by oblique angle deposition at  $\theta = 85^\circ$  without substrate rotation. (a) Top view of the 'fan-out' structure; (b) the cross-sectional view of the 'fan-out' structure; (c) the top view of the 'wall' structure formed on a square lattice; (d) the top view of the 'half-honeycomb' structure formed on a triangular lattice. (e) and (f) are the corresponding side views. The insets in (c) and (d) are the top views of the tungsten pillars arranged on a square lattice and a triangular lattice, respectively.

is related to the incident angle  $\theta$  by a 'tangent rule' [18]. The self-shadowing effect and limited surface diffusion are two dominant mechanisms determining the tilting angle  $\beta$ , the microstructure and the average separation of nanorods. Unfortunately, these three parameters are coupled in oblique angle deposition such that they cannot be changed separately to meet the specific requirements of a desired application. In addition, the number density of nanorods (the number of nanorods per unit area) changes with deposition time due to the competitive nature of oblique angle growth. The shadowing effect favours the growth of longer nanorods that causes a decrease in the number density of nanorods. Also, the fluctuations in the deposition flux (e.g. unstable deposition rates or angular spreads of the incoming particles) make the growth of uniform nanostructures even more difficult. Therefore, large clusters of tilted rods mixed with smaller and shorter rods are common topologies produced.

The lateral separation of the nanorods can be controlled by introducing a template substrate formed by the uniformly separated seed elements that act as nucleation sites for the

growth of nanorods. However, as we observed in our experiment, the nanorods form a 'fan-out' structure due to the anisotropic flux and the lack of shadowing from the direction perpendicular to the plane of incident flux and substrate normal [19–21]. This anisotropic growth eventually results in a fan-out shape, as shown in figure 1(a) top view and (b) side view. At some critical points the larger width nanorods start to touch each other along the direction perpendicular to the incident flux direction ( $y$  direction) while still separated along the incident flux direction ( $x$  direction). This results in the formation of tilted wall-like structures aligned perpendicular to the incident flux plane, as shown in the top views, figures 1(c) and (d), and side views, figures 1(e) and (f) for square and triangular lattices.

In a previous article [22], we demonstrated that the coupling effect between the tilting angle  $\beta$ , the microstructure, and the average separation of nanorods for a large oblique incident angle  $\theta$  deposition on a flat surface without a template can be reduced by introducing an asymmetric substrate rotation. That is within one complete revolution, the substrate

rotates at a rotational speed  $\omega_1$  in a phase sector  $\phi$  and then a higher speed  $\omega_2$  in the rest phase sector  $2\pi - \phi$ . In the current paper, we applied a similar method on templated substrates and we were able to grow well-separated and more uniformly aligned Si nanorods, which cannot be obtained by the conventional approach with *no* substrate rotation. The ‘fan-out’ growth was eliminated by this two-phase substrate rotation method. Si nanorod arrays obtained by this method can be used in various studies of mechanical [23] and electrical properties [24].

## 2. Experimental approach

The setup of our thermal evaporation chamber can be found in our previous articles [22, 25, 26]. Our new design of oblique angle deposition is based on a shadowing effect via a physical self-assembly process. The evaporated atoms arrive at the growing interface at a fixed angle  $\theta$  measured from the substrate normal. The substrate is rotated azimuthally with two different rotational speeds  $\omega_1$  and  $\omega_2$  in each  $360^\circ$  by using a step motor. This ‘two-phase’ rotation of the substrate is described in detail in our previous article [22]. For data presented here the vapour incident angle is  $\theta = 85^\circ$  (with respect to surface normal). The phase sector  $\phi = 135^\circ$  is chosen to get the most tilt nanorods as we discussed previously [22]. The rotational speed  $\omega_1$  is fixed at  $0.0015 \text{ rev s}^{-1}$ , while  $\omega_2$  is fixed at  $0.0075 \text{ rev s}^{-1}$  to give a ratio  $\omega_2/\omega_1 = 5$ . This choice of ratio will be explained later.

The substrates we used in this experiment are patterned Si(100) containing a matrix of tungsten pillars. The tungsten matrix was deposited by chemical vapour deposition (CVD) after patterning holes in a  $1 \mu\text{m}$  thick  $\text{SiO}_2$  layer. The excess tungsten was removed using a chemical mechanical polishing (CMP) technique so that the plugs are flush with the  $\text{SiO}_2$  layer. Two patterns were used for this study:

- (1) tungsten pillars with  $1 \mu\text{m}$  nearest neighbour distance on a 2D square lattice shown as the inset in figure 1(c), and
- (2) tungsten pillars with about  $650 \text{ nm}$  nearest neighbour distance on a 2D triangular lattice, as shown in the inset of figure 1(d).

The  $\text{SiO}_2$  layer was then removed by plasma etching to expose the tungsten pillars. The cone-shape tungsten pillars have a top diameter of  $130 \text{ nm}$  and a bottom diameter of  $360 \text{ nm}$ . The height of each tungsten pillar is about  $450 \text{ nm}$ , as measured by a scanning electron microscopy (SEM). Undoped Si (99.9995%, Alfa Aesar, USA) was evaporated in a graphite crucible by using electron bombardment. The deposition rate was measured by a quartz-crystal microbalance (QCM). The growth rate was  $0.7 \pm 0.03 \text{ nm s}^{-1}$  and the normal thickness was  $4 \mu\text{m}$  in this experiment. The base pressure was about  $8 \times 10^{-5} \text{ Pa}$  and the deposition pressure was less than  $6 \times 10^{-4} \text{ Pa}$ . During depositions, the radiation and the energy transferred from the deposited atoms raised the substrate temperature to about  $80^\circ\text{C}$ .

The grown nanorods were imaged by a field emission scanning electron microscopy (FESEM-6330F, Jeol Ltd, Tokyo, Japan). The samples were cleaved along the plane of the incident flux and the substrate normal (the  $x$  direction) and along the plane perpendicular to it (the  $y$  direction). The

samples were coated with about  $10 \text{ nm}$  thick Pt before being mounted in the SEM chamber. The working distance between a sample and the objective lens was about  $10 \text{ mm}$  during the imaging. The accelerating voltage was  $5 \text{ kV}$  and the current through the tungsten emitter was  $12 \mu\text{A}$ . The resolution of the SEM is  $\sim 1 \text{ nm}$  under these conditions. The tilt angles of individual nanorods and their lengths were measured by drawing lines along the nanorods using Photoshop software (Version 6.0, Adobe Systems Inc., USA). The diameter of a nanorod was measured by drawing a line perpendicular to the axis of a nanorod.

## 3. Results and discussion

As mentioned in the introduction, the rods grown on tungsten pillars by oblique angle deposition without substrate rotation are bundled and expanded (‘fan-out’) in the direction perpendicular to the deposition flux. We can see clearly the initial ‘fan-out’ features, as shown in figures 1(a) and (b), because the growth is limited to one side of the tungsten pillars. Because the deposition flux is static with no change of direction, the growth front is continuous without interruption. So, the growing nanostructures are ‘fan-out’ until touching the shoulder sides (i.e. the  $y$  direction) between two nearest neighbours. The rods touched each other to form a slanted ‘wall’, as shown in figures 1(c) and (d). The top shape is different for the rods grown on different lattices due to the shadowing from neighbours. The top shape of each rod on a square lattice is rectangular, see figure 1(c), while the top shape is ‘half-honeycomb’ for a triangular lattice, see figure 1(d).

In contrast, the nanorods grown by the ‘two-phase’ substrate rotation are uniform and well-aligned, as shown in figure 2. The cross-sectional shapes of the nanorods grown on square and triangular tungsten pillar lattices did not show significant differences as indicated in the SEM top views in figures 2(a) and (b). In the oblique angle deposition with a ‘two-phase’ rotation, the growing interface can be exposed to the incident flux from any angle because the substrate is continuously rotated during a deposition. Therefore some part of the growth front will be interrupted due to the change of the shadowing direction and some part will become a preferred growing front during a rotation. The edge of the growing interface is more liable to be interrupted by shadowing as schematically shown in figure 3. In figure 3(a), the area marked by the thick curved line may be shadowed from the deposition flux. The growth in this region is thus halted. Some part of this area will be exposed to the flux again when the substrate is rotated to an angle as shown in figure 3(b). As a result of the substrate rotation, the nanorods grow directionally without too much ‘fan-out’. Straight nanorods will be formed using this method. On the other hand, for the part of the growth front that is interrupted by a rotation, the surface of the nanorods is not smooth. We can expect the corrugated microstructures on the surface of the rods as shown in the SEM cross-sectional view of the samples cutting along the  $y$  direction in figures 2(e) and (f).

In our ‘two-phase’ rotational method, the tilt angle of the nanorods can be changed through the changing of phase sector  $\phi$  and the ratio of the two rotational speeds  $\omega_1/\omega_2$ . The combination of these two factors and the incident angle  $\theta$  gives an effective deposition angle  $\alpha$  as we obtained from our

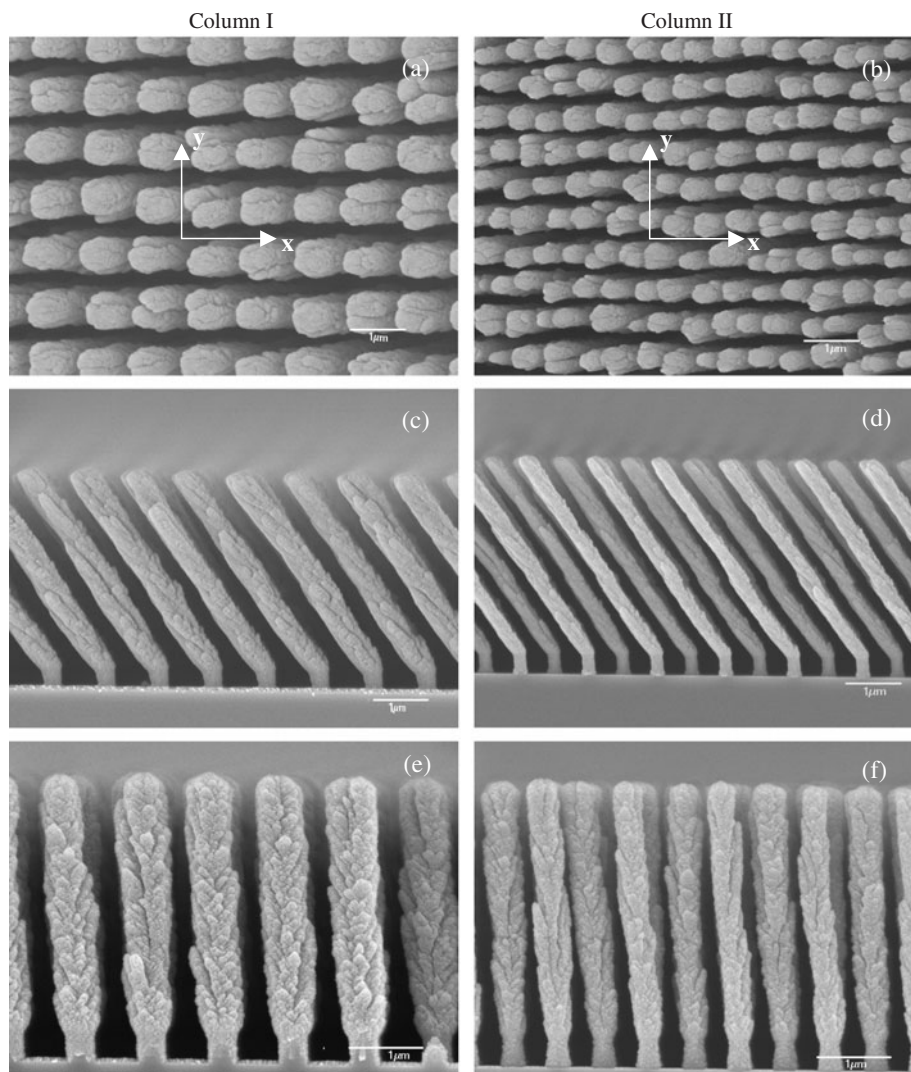


**Figure 2.** SEM images of the nanorods grown by ‘two-phase’ substrate rotation. The nanorods grown on a square lattice are arranged in column I while the nanorods grown on a triangular lattice are in column II. (a) and (b) are the SEM top views; (c) and (d) are the cross-sectional views along the incident vapour direction; (e) and (f) are the cross-sectional views along the direction perpendicular to the vapour flux.

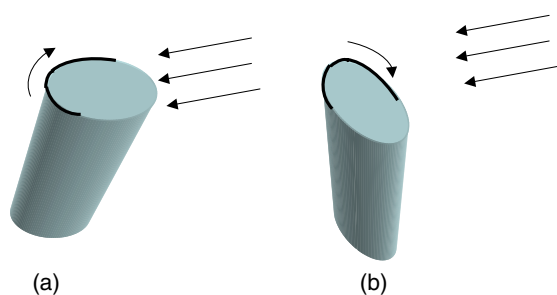


**Figure 3.** Change of the shadowing effect during substrate rotation. The edge marked by the thick line curve in (a) is shadowed, but some part of it is exposed to the flux in (b) when rotated. (This figure is in colour only in the electronic version)

geometrical model [22]

$$\tan \alpha = 2 \frac{\frac{\omega_2}{\omega_1} - 1}{2\pi + (\frac{\omega_2}{\omega_1} - 1)\phi} \tan \theta \sin \frac{\phi}{2}. \quad (1)$$

In our experiments,  $\theta$  is fixed at  $85^\circ$  and  $\phi$  is kept at  $135^\circ$ . Figure 4 shows the change of the effective deposition angle  $\alpha$  as a function of the rotational speed ratio  $\omega_2/\omega_1$ . We found from the plot in figure 4 that  $\alpha \approx 79.5^\circ$  at  $\omega_2/\omega_1 = 5$ . For  $\omega_2/\omega_1 > 5$ ,  $\alpha$  increases very slowly. Hence, we chose  $\omega_2/\omega_1 = 5$  in our experiment to fabricate the tilt nanorods. At a fixed  $\theta$ , one can also calculate the maximum value of  $\alpha$  as a function of  $\phi$  and  $\omega_2/\omega_1$  by taking the derivative of equation (1). However, with fixed  $\theta$  and  $\phi$ ,  $\alpha$  changes by less than 1 when we change  $\omega_2/\omega_1$ . The tilt angles were measured with respect to the substrate normal for nanorods grown on a flat Si(100) substrate and on the patterned tungsten pillars. On a flat surface, the measured tilt angle is  $\beta = 36.0^\circ \pm 0.5^\circ$ . For nanorods grown on the tungsten pillars in the triangular lattice and square lattice,  $\beta = 35.7^\circ \pm 0.3^\circ$  and  $\beta = 35.7^\circ \pm 0.4^\circ$ , respectively. These data imply that the geometrical model we developed is universal for the two templated substrates that we tested. The tilt angle  $\beta$  of the nanorods grown on a bare surface relates to  $\alpha$  in the empirical tangent rule for

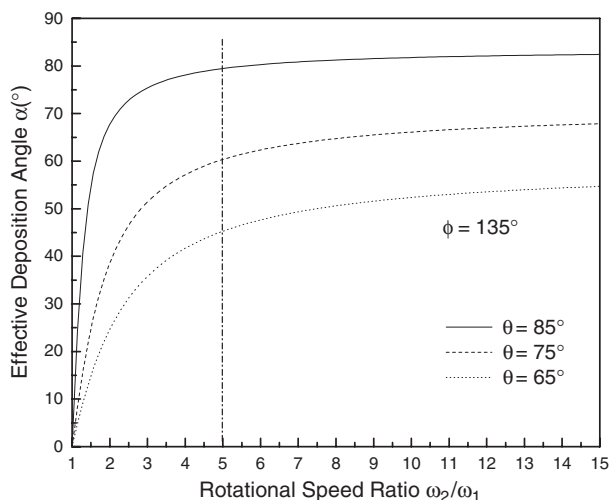


**Figure 4.** The effective deposition angle  $\alpha$  as a function of ratio of substrate rotational speeds  $\omega_2/\omega_1$ . The phase sector is fixed at  $\phi = 135^\circ$  while the incident vapour angles are  $\theta = 65^\circ, 75^\circ$  and  $85^\circ$ .

small  $\alpha$  ( $<50^\circ$ ) [18, 27],

$$\tan \beta = \frac{1}{2} \tan \alpha, \quad (2)$$

or the cosine rule as for large  $\alpha$  [28],

$$\beta = \alpha - \arcsin\left(\frac{1 - \cos \alpha}{2}\right). \quad (3)$$

However, both the tangent rule and cosine rule cannot predict the measured tilt angle  $\beta$  of rods grown under the ‘two-phase’ substrate rotation. As a reference, the nanorods have larger tilt angles  $\beta = 53.6^\circ \pm 0.5^\circ$  when deposited at  $\theta = 85^\circ$  on patterned tungsten pillars by oblique angle deposition without substrate rotation. This measured tilt angle  $\beta = 53.6^\circ \pm 0.5^\circ$  can be predicted using the cosine rule. The tangent rule is rooted in the surface diffusion of adatoms and self-shadowing effects [29]. When a substrate is rotated, the nanorods might tilt less because of the changing shadowing direction. Thus we can revise the tangent rule in equation (2) to  $\tan \alpha = 2 \tan(\beta)$ , which yields a better fit of the tilt angle in the ‘two-phase’ rotation case.

The length and the diameter of the nanorods were measured from SEM images. The average length of the nanorods grown on a square lattice and a triangular lattice are  $4206.8 \pm 45.1$  and  $4212.7 \pm 23.9$  nm, respectively. The nanorods grown on a triangular lattice are smaller than those on a square lattice because the distance of the nearest neighbours is about 350 nm smaller than the square lattice. The measured diameter of the nanorods grown on a triangular lattice is  $304.5 \pm 20.0$  nm in the  $x$  direction while the diameter is  $438.3 \pm 41.5$  nm in the  $y$  direction. The nanorods grown on the square lattice also show the anisotropic characters which have the diameters of  $468.1 \pm 35.9$  nm in the  $x$  direction and  $687.7 \pm 59.2$  nm in the  $y$  direction.

#### 4. Conclusion

In summary, we have fabricated well-aligned tilted nanorods on tungsten pillars on square and triangular lattices by oblique

angle deposition with ‘two-phase’ rotation. The tilt angle of the nanorods is close to  $36^\circ$  which is not expected from either a tangent rule or a cosine rule. Our new method has advantages over the traditional oblique angle deposition in that the new method can provide more uniform growth of tilted structures by eliminating the ‘fan-out’ effect. It is also observed that one can create well separated 3D rods. We also showed in the SEM images that the diameter of a growing rod saturates quickly. This property offers the flexibility of fabricating nanorods to any desired length. Our work may open new opportunities for creating uniform novel structures by introducing more rotational phase sectors.

#### Acknowledgments

This work was supported by the NSF and the Semiconductor Research Corporation (SRC).

#### References

- [1] Dekker C 1999 *Phys. Today* **52** 22
- [2] Hu J, Odom T W and Lieber C M 1999 *Acc. Chem. Res.* **32** 435
- [3] Cui Y and Lieber C M 2001 *Science* **291** 851
- [4] Chang C S, Chattopadhyay S, Chen L C, Chen K H, Chen C W, Chen Y F, Collazo R and Sitar Z 2003 *Phys. Rev. B* **68** 125322
- [5] Wang Q H, Corrigan T D, Dai J Y, Chang R P H and Krauss A R 1997 *Appl. Phys. Lett.* **70** 3308
- [6] Huang M H, Mao S, Feick H, Yan H, Wu Y, Kind H, Weber E, Russo R and Yang P 2001 *Science* **292** 1897
- [7] Poborchii V, Tada T, Kanayama T and Moroz A 2003 *Appl. Phys. Lett.* **82** 508
- [8] Tao A, Kim F, Hess C, Goldberger J, He R, Sun Y, Xia Y and Yang P 2003 *Nano Lett.* **3** 1229
- [9] Wong E W, Sheehan P E and Lieber C M 1997 *Science* **277** 1971
- [10] Braiman Y, Barhen J and Protopopescu V 2003 *Phys. Rev. Lett.* **90** 094301
- [11] Otitii T, Niklasson G A, Svedlindh P and Granquist C G 1997 *Thin Solid Films* **307** 245
- [12] Otitii T 2001 *J. Mater. Sci. Lett.* **20** 845
- [13] Otitii T 2003 *J. Mater. Sci. Lett.* **38** 1315
- [14] Smith D O, Cohen M S and Weiss G P 1960 *J. Appl. Phys.* **31** 1755
- [15] Metzendorf W and Wiehl H E 1966 *Phys. Status Solidi* **17** 285
- [16] Dick B, Brett M J and Smy T 2003 *J. Vac. Sci. Technol. B* **21** 2569
- [17] Abelmann L and Lodder C 1997 *Thin Solid Films* **305** 1
- [18] Niuwenhuizen J M and Haanstra H B 1966 *Philips Tech. Rev.* **27** 87
- [19] Meakin P and Krug J 1990 *Europhys. Lett.* **11** 7
- [20] Meakin P and Krug J 1992 *Phys. Rev. A* **46** 3390
- [21] Karabacak T, Singh J P, Zhao Y-P, Wang G-C and Lu T-M 2003 *Phys. Rev. B* **68** 125408
- [22] Ye D-X, Zhao Y-P, Yang G-R, Zhao Y-G, Wang G-C and Lu T-M 2002 *Nanotechnology* **13** 615
- [23] Hartland G V, Min Hu, Wilson O and Mulvaney P 2002 *Proc. SPIE* **4934** 52
- [24] Li L and Alivisatos A P 2003 *Phys. Rev. Lett.* **90** 097402
- [25] Zhao Y-P, Ye D-X, Wang G-C and Lu T-M 2002 *Nano Lett.* **2** 351
- [26] Zhao Y-P, Ye D-X, Wang P-I, Wang G-C and Lu T-M 2002 *Int. J. Nanosci.* **1** 87
- [27] Dirks A G and Leamy H J 1977 *Thin Solid Films* **47** 219
- [28] Trait R N, Smy T and Brett M J 1993 *Thin Solid Films* **226** 196
- [29] Abelmann L and Lodder C 1997 *Thin Solid Films* **305** 1